

Quantification of Flexibility of a District Heating System for the Power Grid

Xiandong Xu, Quan Lyu, Meysam Qardran, Jianzhong Wu*

Abstract— District heating systems (DHS) that generate/consume electricity are increasingly used to provide flexibility to power grids. The quantification of flexibility from a DHS is challenging due to its complex thermal dynamics and time-delay effects. This paper proposes a three-stage methodology to quantify the maximum flexibility of a DHS. The DHS is firstly decomposed into multiple parallel subsystems with simpler topological structures. The maximum flexibility of each subsystem is then formulated as an optimal control problem with time delays in state variables. Finally, the available flexibility from the original DHS is estimated by aggregating the flexibility of all subsystems. Numerical results reveal that a DHS with longer pipelines has more flexibility but using this flexibility may lead to extra actions in equipment such as the opening position adjustment of valves, in order to restore the DHS to normal states after providing flexibility. Impacts of the supply temperature of the heat producer, the heat loss coefficient of buildings and the ambient temperature on the available flexibility were quantified.

Index Terms— District heating system, flexibility, optimization, power grid, transport delay.

NOMENCLATURE

CHP	Combined heat and power
DER	Distributed energy resources
DHS	District heating system
TCL	Thermostatically controlled loads
t	Time
t_0	Start time of flexibility provision
t_b	The duration that a building can sustain above the minimum temperature without heat supply
P_{flexis}	The flexibility of an individual system
\bar{P}_{flexis}	The maximum flexibility of an individual system
P_{actual}	The magnitude of electricity that an individual system imports from/exports to the power grid
$P_{desired}$	The electricity generation/consumption of an individual system during normal operation
t_{min}	Minimum duration for flexibility provision
T	Temperature of the heating network and buildings
N_T	The number of states in the DHS
N_p	The number of pipelines
τ_j	The transport delay of pipeline j

Q_h	Heat producer output
Q_d	The desired heat producer output
Q_{flexis}	The allowance of mismatch between Q_h and Q_d
T_{amb}	The outdoor temperature
P_{flexis}^{demand}	Flexibility demand of the power grid
γ_{h2p}	Heat to power ratio of the coupling unit
\underline{Q}_h	Lower bound of heat producer output
\overline{Q}_h	Upper bound of heat producer output
T_f	The temperature of the heating network
\underline{T}_f	Lower bound of T_f
\overline{T}_f	Upper bound of T_f
T_b	Temperature of buildings
\underline{T}_b	Lower bound of T_b
\overline{T}_b	Upper bound of T_b
t_{flexis}	Duration of flexibility provision
Ω_{dhs}	Constraints of the heating network and buildings
ξ	The initial state of the DHS
m_0	The flow rate at the producer side
m_i	The flow rate at the demand side
N_s	The number of heat substations
$v_{b,i}$	The flow velocity of branch pipeline i
$A_{t,k}$	Cross-sectional area of trunk pipeline k
$A_{b,i}$	Cross-sectional area branch pipeline i
$l_{t,k}$	Length of trunk pipeline k
$l_{b,i}$	Length of branch pipeline i
v_k	Flow velocity of water in trunk pipeline k
τ_{di}	Transport delay of subsystem i
$Q_{d,i}$	Desired heat supply to the i^{th} subsystem
$\underline{Q}_{d,i}$	Lower bound of $Q_{d,i}$
$\overline{Q}_{d,i}$	Upper bound of $Q_{d,i}$
$T_{1,o,i}^b$	Output temperature at the primary side of the building heat exchanger in subsystem i
$T_{2,o,i}^b$	Output temperature at the secondary side of the building heat exchanger in subsystem i
T_s^p	Supply temperature at the secondary side of the producer heat exchanger
\underline{T}_s^p	Lower bound of T_s^p
\overline{T}_s^p	Upper bound of T_s^p

This work was supported in part by FLEXIS (Flexible Integrated Energy Systems) and the UK Engineering and Physical Sciences Research Council (EPSRC) EPSRC for funding “Maximizing flexibility through multi-scale integration of energy systems” project (EP/S001492/1). FLEXIS is part-funded by the European Regional Development Fund (ERDF), through the Welsh Government.

X. Xu, M. Qardran, and J. Wu are with the School of Engineering, Cardiff University, Cardiff, CF24 3AA UK (e-mail: xux27@cardiff.ac.uk; qardranm@cardiff.ac.uk; wuj5@cardiff.ac.uk).

Q. Lyu is with the School of Electrical Engineering, Dalian University of Technology, Liaoning, 116024 China (e-mail: q.lyu@foxmail.com).

$T_{b,i}$	Equivalent building temperature of subsystem i
$\underline{T}_{b,i}$	Lower bound of $T_{b,i}$
$\overline{T}_{b,i}$	Upper bound of $T_{b,i}$
T_{env}	Surrounding temperature of pipelines
$Q_{h,i}$	The i^{th} heat producer output
n_u	Number of intervals for the discretized equations
F_{flexis}	The maximum duration of a flexibility service
n_{flex}	The dimension of the discretized DHS model
$n_{p,j}$	The number of discretized steps of the j^{th} delay
T_{in}	Inlet temperature of the pipeline.
T_{out}	Output temperatures of the pipeline
f_p	Thermal model of the pipeline.
λ	Overall heat transfer coefficient of the pipeline
c_w	Specific heat of water.
T_r^p	Return temperature at the secondary side of a heat exchanger
\dot{m}_p	Flow rate at the secondary side of a heat exchanger
$T_{1,i}^b$	Inlet temperature at the primary side of the building heat exchanger.
$T_{1,o}^b$	Output temperature at the primary side of the building heat exchanger.
$T_{2,i}^b$	Inlet temperature at the secondary side of the building heat exchanger.
$T_{2,o}^b$	Output temperatures at the secondary side of the building heat exchanger.
m_1^b	Mass of flow inside the primary circuit of the building heat exchanger.
m_2^b	Mass of flow inside the secondary circuit of the building heat exchanger.
H^b	Heat loss coefficient of the building.
C_b	Heat capacity of the building
\dot{m}_b	Flow rate at the secondary side of the building heat exchanger
k_l	Overall heat loss coefficient of the building

I. INTRODUCTION

THE integration of intermittent renewable energy sources poses severe challenges to power grids, particularly to the balance of electricity supply and demand. The short-term imbalances may lead to not only technical issues such as significant frequency fluctuations but also the volatility of electricity prices. For instance, in May 2017, the electricity price in Great Britain reached £1,510/MWh due to a sudden drop of wind power along with the outage of an interconnector [1]. This figure is almost 30 times higher than the average wholesale electricity price in Great Britain. To mitigate the adverse impacts of variable renewable generation on the operation of power grids, additional forms of flexibility provided by energy storage and demand response are required. Such flexibility can help power grids managing periods of high variability in electricity demand and supply. Due to high capital costs and potential environmental impacts, grid-scale electrical storage is not widely used. A more economical solution is to use energy storage that already exists in gas and heat supply

systems [2]. To employ this solution, the concept and architecture of integrated energy management system are presented in [3], which for the first time truly breaks down the walls between different energy systems and implements a highly coordinative management and control of multi-energy flow in real applications. Hereby in the context of energy system integration, the flexibility refers to the ability that an energy system can adjust and maintain its electricity generation/consumption within a given period so as to support the operation of power grids [4].

A. Sources of Flexibility

The heat sector is among the major candidates for providing flexibility to power grids [5][6] if the heat production is coupled to electricity consumption/generation [7]. Through demand response, buildings supplied by heat pumps or electric heaters can provide flexibility to power grids. Such flexibility has been widely embraced by utilities [8]. In a district heating system (DHS), besides the available flexibility from adjusting heat loads of buildings [9], it is possible to procure flexibility from the thermal inertia of water inside pipelines. The flexibility is then transferred to power grids via heat producers, such as power to heat units [10] or combined heat and power (CHP) units [11]. This flexibility is provided by controlling the electricity consumption/generation of heat producers in coordination with the pipeline network [12] and buildings [13]. In CHP systems, reciprocating engines and aero-derivative gas turbines are often used for producing electricity and heat. They have fast ramp rates and thus are feasible and flexible for providing ancillary services [14]. For example, if a CHP is used as the heat producer and frequency response is chosen as the flexibility service, the CHP will increase its electricity generation when a low-frequency response is activated. Although one CHP unit has a limited capacity, the frequency can be restored via aggregated response from multiple CHP units following the activation signal from power grids. A flexible CHP system at Princeton University which was designed to support campus' heat and electricity needs, has been employed to enable frequency regulation [15].

In Europe where DHSs are well developed, the DHSs provide flexibility to power grids by participating in energy and ancillary services markets [16]. Through these markets, DHS owners can access to extra revenue streams, which give them incentives to release their flexibility. In a case study in Belgium [17], it has been shown that a total cost decrease of 5% could be achieved by using CHP to provide balancing services. Exploiting flexibility from the heat sector is also a cost-effective solution to facilitate the integration of renewable energy [18] and mitigating power grid constraints [19].

B. Challenges of Flexibility Quantification

Traditionally, DHSs are operated to follow local heat demand, which changes relatively slowly. Operators control the supply temperature and the flow velocity of water in pipelines to meet the heat demand [20]. When a DHS is used to support the operation of power grids, more frequent adjustments to the electricity generation/consumption of the heat producer are

required. These adjustments consequently affect the DHS operation. The heat supply fluctuations are then propagated to the whole DHS [21]. To provide more flexibility, the DHS may be pushed to its operational limits, which include comfort level limits of households and temperature limits of pipeline networks. A key challenge is how to quantify the maximum flexibility of a DHS considering all these limits.

The maximum flexibility of a DHS relates to the control of heat supply and demand. In [22], a region-based method is proposed to estimate the flexibility of DHSs, which reduces the energy cost and wind curtailment without relying on detailed models of DHSs. In [23], optimal control of a system of CHP, furnace, and batteries is used to exploit the flexibility of a hybrid energy system. However, the thermal inertia of buildings and water in pipelines as well as the transport delay of heat are not considered. In [11], the CHP operation is optimized based on an aggregated load model. The slow flow velocity in pipelines leads to considerable transport delays in the heat supply of DHS, particularly when there is a long distance between heat producers and consumers [24]. These delays give challenges to solution algorithms for the flexibility estimation of DHSs, due to additional variables in describing delayed states.

In [25]-[26], the flexibility from heat transfer process is considered for the dispatch of coupled power grid and DHS based on steady-state models. From the viewpoint of DHS operation, provision of flexibility also needs to ensure the security of heat supply in short terms. A more detailed model is required to quantify the maximum flexibility. In [27], a geometric approach is proposed to aggregate the flexibility of thermostatically controlled loads (TCLs), which are represented as ON/OFF units. The regulation of individual TCL does not affect the flexibility of other TCLs. For the DHS, the geometric approach needs to be enhanced by incorporating continuous behavior of heating systems and mutual impacts of regulation of various TCLs via pipeline networks. In [28], the flexibility of multiple distributed energy resources (DERs) with known flexibility domains is aggregated. However, the impact of the heating systems on the DERs as well as dynamic evolution of flexibility is neglected.

Note that the market conditions of power grids also play a key role in exploiting the flexibility. Utilities have to pay flexibility providers to obtain services, when an imbalance in electricity supply and demand occurs. Provision of flexibility services is based on capability of flexibility providers. Operators of the DHS can decide how much flexibility will be sold to power grids. However, the operators must know the maximum amount of flexibility that a DHS can provide in order to avoid disrupting heat supply to customers.

C. Main Contributions of This Paper

This paper focuses on a radial DHS supplied by a heat producer that couples a power grid and the DHS. Main work includes: 1) A model-based method was proposed to help DHS owners to evaluate their maximum change of electricity generation/consumption for flexibility provision under given operating conditions; 2) Evaluation criteria were defined for

utility operators to screen flexibility providers from existing or new DHSs that have intentions to support the power grid; 3) Key factors that affect the flexibility of DHS were identified, which can support DHS owners in their investment decisions on flexibility enhancement. In the case study, only a CHP is studied as the coupling unit. The proposed method is applicable to DHSs supplied by other units that connect to the power grid.

II. DESCRIPTION OF OPERATIONAL FLEXIBILITY

A. Definition of Flexibility for the Power Grid

For a given time t , the flexibility of an individual system $P_{flexis}(t)$ can be expressed as

$$P_{flexis}(t) = P_{actual}(t) - P_{desired}(t) \quad (1)$$

where $P_{actual}(t)$ represents the magnitude of electricity that the individual system imports from/exports to the power grid during the flexibility provision period. $P_{desired}(t)$ represents the electricity generation/consumption of the individual system during the normal operation. The DHS provides upward flexibility when $P_{flexis}(t) > 0$, and downward flexibility when $P_{flexis}(t) < 0$.

The flexibility can be used for peak shaving or ancillary services, which have different duration requirements. For example, in Great Britain, secondary frequency response should sustain for a minimum of 30 minutes [29] while short-term operating reserve should sustain for a minimum of 2 hours [30].

Assume that \bar{P}_{flexis} is the maximum flexibility that a DHS can provide within a minimum duration t_{min} , then the flexibility requested by the power grid satisfies

$$\forall t \in (t_0, t_0 + t_{min}], |\bar{P}_{flexis}| \geq P_{flexis}(t) \quad (2)$$

B. Flexibility Provision from a DHS

1) Description of the DHS

This paper studies a DHS with a radial structure, which is widely used in practice. Main components of the DHS include a coupling unit, a network of pipelines, heat substations and buildings as shown in Fig. 1. The coupling unit refers to energy conversion technologies that link two or more energy systems. In this paper, the coupling unit is the heat producer, which could be a CHP or a power to heat unit such as an electric heater or a heat pump that links the DHS to the power grid. A CHP produces electricity and heat simultaneously, while a power to heat unit produces heat and consumes electricity. The coupling unit is necessary for using the flexibility of DHS to support the power grid. If a heat producer like a gas boiler is used, changing the heat supply of DHS has minor impact on the power grid. Then no flexibility can be provided by the DHS to the power grid.

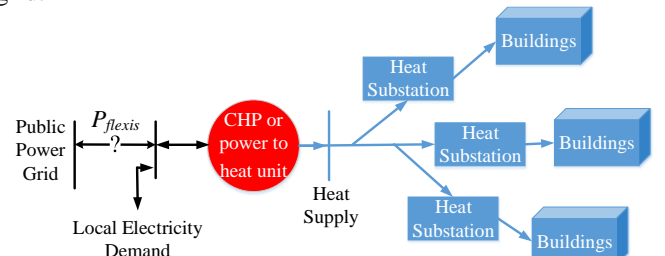


Fig. 1 Schematic representation of a DHS coupled with the power grid.

2) Control of the Heat Producer to Support the Power Grid

Under normal operations, the heat producers are controlled to meet the heat demand of buildings. The electricity (generation for CHP and consumption for the power to heat units) is a by-product and not controlled. If the heat demand changes, the by-product electricity will vary. When used for supporting the power grid, the control signal of the heat producer is replaced by a new control signal generated according to the requirements of the power grid. Specifically, the control signal is obtained as follows:

1) If the CHP is used as a heat producer: Without supporting the power grid, the CHP is operated at the heat-driven mode. Using a CHP driven by gas engines as an example, the heat output is controlled by regulating the fuel input of gas engines. The setpoint of fuel input is generated according to the variation of supply temperature of the DHS [31]. When supporting the power grid, the CHP is switched to the electricity-driven mode and will not follow the heat demand. This mode allows the supply temperature to deviate from the setpoint as long as all temperatures of the DHS are within limits. It has been shown in [15] that this mode switching can be achieved within the time required for frequency support to the power grid.

2) If a power to heat unit is used as the heat producer: Without supporting the power grid, the unit is used for maintaining the supply temperature of the DHS at given levels. The electricity consumption is determined by the heat demand. When supporting the power grid, the heat output is adjusted to generate more/less heat until the electricity consumption of the power to heat unit meets the requirement of the power grid.

The change of by-product heat output may result in a mismatch between heat supply and demand, which can be accommodated by the thermal inertia of buildings and water in pipelines for a certain period.

3) Availability of the Flexibility from DHS to the Power Grid

Assuming that the water flow in pipelines is not adjusted when providing flexibility, then the dynamic behavior of the DHS is expressed as (details are given in Appendix A)

$$\dot{\mathbf{T}}(t) = f(t, \mathbf{T}(t), \mathbf{T}(t - \tau_1), \mathbf{T}(t - \tau_2), \dots, \mathbf{T}(t - \tau_{N_p}), Q_h, \mathbf{T}_w) \quad (3)$$

where \mathbf{T} represents the state variables, which refer to the temperatures of the heating network and buildings, $\mathbf{T} \in \mathbb{R}^{N_T}$. N_T represents the total number of states in the heating network and buildings. \mathbf{T}_w represents the surrounding temperature of the pipelines (e.g. soil temperature) T_{env} and the outdoor temperature of the buildings T_{amb} , $\mathbf{T}_w = [T_{env} T_{amb}] \in \mathbb{R}^2$. $f: \mathbb{R} \times \mathbb{R}^{(N_p+1) \times N_T} \times \mathbb{R} \rightarrow \mathbb{R}^{N_T}$ are given functions. τ_j represents the transport delay of pipeline j , $j=1, 2, \dots, N_p$. N_p represents the number of pipelines. For simplicity, the pipelines are sorted based on the length of their heat transport delays in ascending order, $\tau_1 < \tau_2 < \dots < \tau_{N_p}$. Q_h represents the output of heat producer.

The flexibility of a DHS lies in the allowance of mismatch Q_{flexis} between Q_h and the desired heat producer output Q_d (see Appendix B for details).

The electricity generation/consumption and the heat output of heat producers are constrained by heat to power ratio γ_{h2p}

[32]. When providing flexibility, changes in the output of heat producer Q_{flexis} can be obtained by

$$Q_{flexis} = P_{flexis} \gamma_{h2p} \quad (4)$$

As an extension of (1), heat producer output when providing flexibility can be described by

$$Q_h = Q_d + Q_{flexis} \quad (5)$$

To provide flexibility to the power grid, the following criteria should be satisfied.

- (C1) A coupling unit such as CHP or power to heat unit exists between the power grid and the DHS;
- (C2) The coupling unit between the power grid and the DHS is controllable. Either ON/OFF switching or output adjustment is allowed to the coupling unit;
- (C3) Flexibility requirement of the power grid P_{flexis}^{demand} , Q_{flexis} and heat to power ratio of the coupling unit γ_{h2p} satisfy $P_{flexis}^{demand} * Q_{flexis} / \gamma_{h2p} > 0$.

For a small-scale CHP, γ_{h2p} can be considered as a positive constant. For large-scale CHP plants with extraction condensing turbines, γ_{h2p} can be adjusted within a range [32]. The upper and lower bounds of γ_{h2p} may vary as the CHP electricity output changes. If a CHP is operated at its maximum output, $Q_{flexis} \leq 0$, the DHS could only provide downward flexibility. For a power-to-heat unit, γ_{h2p} is equal to the efficiency of the unit multiplied by -1, which is negative.

4) Limitations of Flexibility Provision

The operation of the DHS is limited by

a) *Heat producer output*: Q_h is limited by \underline{Q}_h and \bar{Q}_h namely the lower and upper bounds of heat producer output.

b) *Heating network temperature*: To meet the heat demand of the DHS, the temperature of water flow in pipelines should be within the lower and the upper limits $[\underline{T}_f, \bar{T}_f]$. The upper limit is set up to avoid water vaporization, which is critical for the security of the DHS. The lower limit is mainly set up by operators to maintain the normal operation.

c) *Building temperature*: The building temperature should be within occupants' comfort zone, i.e. within the lower and the upper limits $[\underline{T}_b, \bar{T}_b]$.

d) *Transport delay*: When a flexibility provision process is over, the extra/shortage of heat in the supply pipelines may lead to increase or decrease in building temperatures for another period τ_d . Fig. 2 shows the impact of transport delay on the DHS with one producer and one consumer as an example.

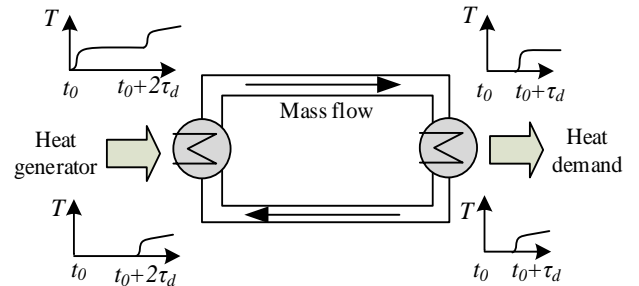


Fig. 2. The impact of transport delay on the DHS.

When the heat producer output at t_0 increases, the supply temperature changes from T_{in} to T'_{in} . T'_{in} can be maintained

until $t = t_0 + 2\tau_d$, when the heated mass flow at t_0 goes back to the supply side. As the temperature of the return water increases, subsequently T'_{in} will rise to a new value if the heat producer output is not properly adjusted. For the heat demand, this rise starts at $t = t_0 + \tau_d$, and then occurs every $2n\tau_d$, where n is obtained by rounding off $[t/\tau_d]$. These jumps in the states could result in a sudden flexibility loss with a τ_d delay. For a given flexibility service period t_{flexis} , the temperature of the whole system needs to be within the above operating constraints, $\forall t \in (t_0, t_0 + t_{flexis} + \tau_d]$.

In real-time operation, the output of the heat producer Q_h is constrained to leave headroom above for providing upward or downward flexibility when needed. Additionally, the available duration of the DHS for flexibility provision needs to be estimated to ensure that the DHS can sustain for the minimum period required for flexibility provision.

C. Problem Formulation for Maximum Flexibility Provision

When the flexibility of an individual system is used to acquire more profits in a market, a maximum flexibility provision is preferred. Considering that the demand for flexibility can be either positive or negative, the maximum flexibility of a DHS is thus expressed as upward and downward boundaries. Referring to [33], the maximum flexibility within a period t_{flexis} can be formulated as an optimal control problem with state constraints.

$$\begin{cases} \text{Maximize} & \int_0^{t_{flexis}} |Q_{flexis}(t)| dt \\ \text{subject to} & \\ (3) & \\ T(t) \in \Omega_{dhs}, \text{ a.e. } t \in [0, t_{flexis} + \tau_{np}] & \\ Q_h \leq Q_h \leq \bar{Q}_h, \text{ a.e. } t \in [0, t_{flexis}] & \end{cases} \quad (6)$$

where Ω_{dhs} represents operating constraints of the heating network and buildings, $\Omega_{dhs} = \{\mathbf{T}(t) = [\mathbf{T}_f(t), \mathbf{T}_b(t)], \mathbf{T}_f \leq \bar{\mathbf{T}}_f, \mathbf{T}_b \leq \bar{\mathbf{T}}_b\}$. $\xi(t) \in \mathbb{R}^m$ represents the initial state of the DHS, $t \in [-\tau_{Np}, 0]$.

One way of solving the optimal control problem with time delay in states is to discretize the equations and convert the problem to a constrained optimization problem. In practice, a DHS may have more than one pipelines with various lengths, which will significantly bring in different transport delays and increase the computational burden (see Appendix C) and thus requires a simplified method.

III. QUANTIFICATION OF MAXIMUM FLEXIBILITY

This paper considers the DHS with a central control system on the producer side. The heat supply of the DHS is maintained by adjusting the supply temperature, which will affect all subsystems. If any subsystem reaches its operating boundary, flexibility provision of the whole DHS will be limited. A three-stage method is proposed to estimate the flexibility of the DHS (see Fig. 3).

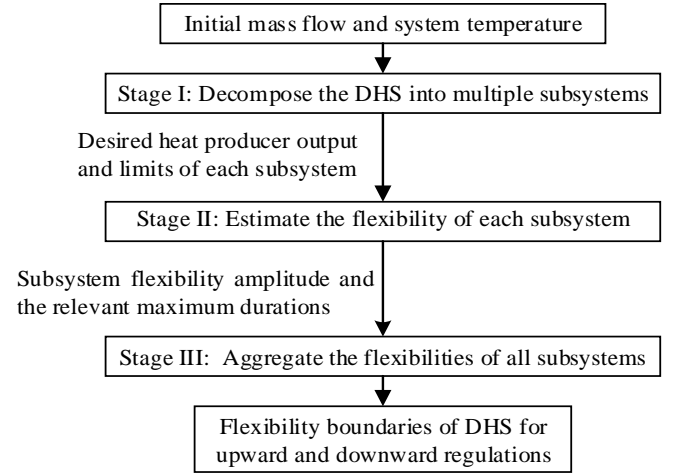


Fig. 3. Flowchart of the proposed flexibility quantification method.

A. Equivalent DHS Model for Flexibility Analysis

To address the complexity involved in the flexibility quantification process, this paper proposes an equivalent model which decomposes the original DHS into multiple subsystems with a single-producer single-consumer structure.

$$m_0 = \sum_{i=1}^{N_s} m_i \quad (7)$$

where N_s represents the number of heat substations.

The flow velocity of branch pipeline i is calculated by $v_{b,i} = m_i / (\rho_w A_{b,i})$. For a radial pipeline network, the water flow of a trunk pipeline that goes into a node is equal to the total flow of branch pipes and other trunk pipes, which act as the outlet of the same node [34]. The flow rate of trunk pipeline k is $m_{t,k} = \sum_{i=k}^{N_s} m_i$. The flow velocity of trunk pipeline k is expressed as

$$v_k = \frac{\sum_{i=k}^{N_s} m_i}{\rho_w A_{t,k}} \quad (8)$$

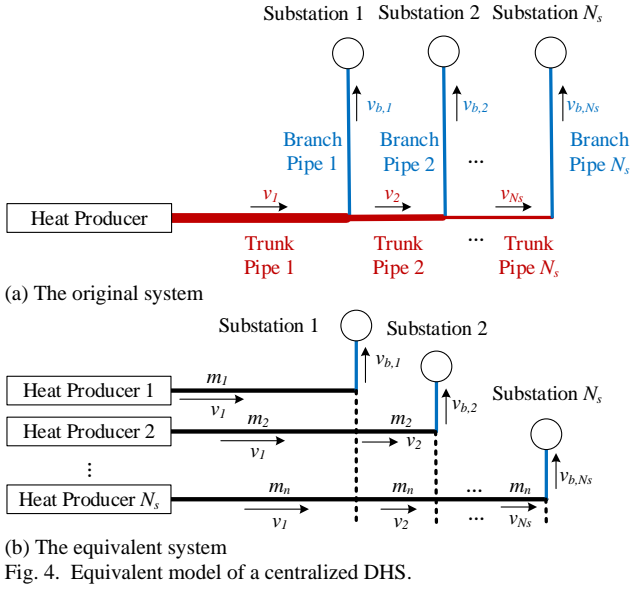
where $A_{t,k}$ and $A_{b,i}$ represent cross-sectional areas of trunk pipeline k and branch pipeline i . ρ_w represents the water density.

Assume that the water inside the pipelines is incompressible the transport delay of water flow inside a pipeline represents the time required for the water that moves from one end to the other end of the pipeline [35]. Then the transport delay of subsystem i can be calculated by

$$\tau_{di} = \frac{l_{b,i}}{v_{b,i}} + \sum_{k=1}^i \frac{l_{t,k}}{v_k} \quad (9)$$

where $l_{t,k}$ and $l_{b,i}$ represent the length of trunk pipeline k and the length of branch pipeline i .

Mathematically, the DHS can be decomposed into N_s equivalent subsystems with a single-producer single-consumer structure as shown in Fig. 4. The flow rate in each subsystem is equal to the primary flow rate of the relevant substation in the original system. The flow velocity of trunk pipeline k of each subsystem is equal to the flow velocity of the original pipeline k . The friction factor and the heat loss factor of the decomposed pipelines are extracted from the original pipeline. The obtained parameters ensure that the decomposed systems can reflect hydraulic and thermal behaviors of the original system. Details of the parameter extraction process are given in Appendix D.



For the DHS studied in this paper, the flow rates inside pipelines are controlled to be constant during the flexibility provision period. The excess/deficit heat producer output for flexibility provision is transported to various demands. For a given amplitude of flexibility demand (adjustment in electricity generation/consumption), the maximum duration of flexibility provision from a DHS is decided by the time required for the building temperature or the supply temperature to go beyond the allowable range. So, this duration is determined by physical characteristics of buildings and water in pipelines. The decomposition method doesn't affect flexibility estimation results. Moreover, the decomposition analysis doesn't directly change the control system but brings in extra steps to flexibility analysis. The extra steps reduce the calculation burden for flexibility estimation of the original DHS. The results can support the decision-making of the operator for adjusting the power generation/consumption of the heat producer.

To ensure that the heat in the DHS is used efficiently, the return temperature at the primary side of the heat substation is controlled to be operated at its minimum value, which can be achieved by adjusting the flow rate during the normal operation. Therefore, the heat supplied to demand is proportional to the flow rate of water transported to the heat substation [36]. The desired heat supply to the i^{th} subsystem $Q_{d,i}$ can be approximated by

$$Q_{d,i} = \frac{m_i}{\sum_{i=1}^{N_s} m_i} Q_d \quad (10)$$

1) Subsystem Model

The behavior of the decomposed subsystems can be described by a power-interface-thermal system model as shown in Fig. 5. The heat is injected into the primary network through a producer heat exchanger. The secondary network is studied as a part of the equivalent building which extracts heat from the heating network through a building heat exchanger.

Based on the component model in Appendix A, the model of subsystem i can be expressed as

$$\dot{T}_i(t) = \mathbf{A}_0 T_i(t) + \mathbf{A}_1 T_i(t - \tau_{d,i}) + \mathbf{B} Q_{h,i} + \mathbf{E} T_w \quad (11)$$

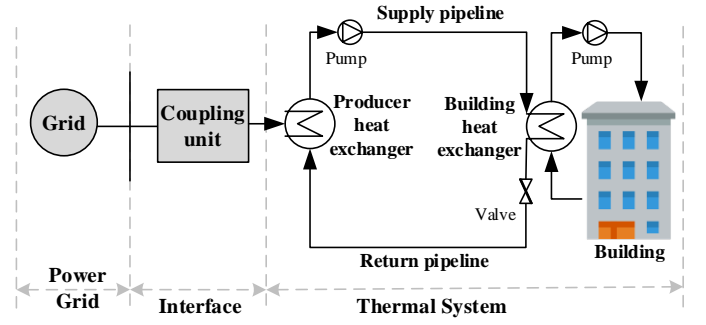


Fig. 5. Schematic of a subsystem of DHS coupled with the power grid.

where $T_i(t) = [T_s^p T_{1,o,i}^b T_{2,o,i}^b T_{b,i}]^T$, $T_w = [T_{env} T_{amb}]^T$. T_s^p represents the supply temperature at the secondary side of the producer heat exchanger. $T_{1,o,i}^b$ represents the outlet temperature at the primary side of the heat exchanger of the equivalent building in subsystem i . $T_{2,o,i}^b$ represents the outlet temperature at the secondary side of the heat exchanger of the equivalent building. $T_{b,i}$ represents the temperature of the equivalent building. $Q_{h,i}$ represents the i^{th} heat producer output. \mathbf{A}_0 , \mathbf{A}_1 , \mathbf{B} and \mathbf{E} can be found in Appendix E.

2) Flexibility Quantification of Subsystems

For a radial DHS, the supply temperature is a key state in the DHS control. The supply temperature at the secondary side of the producer heat exchanger T_s^p is limited by

$$\underline{T}_s^p \leq T_s^p \leq \bar{T}_s^p \quad (12)$$

where \underline{T}_s^p and \bar{T}_s^p represent the lower and the upper bounds of T_s^p .

Moreover, the building temperature satisfies

$$\forall t \in (0, t_{flexis} + \tau_{d,i}], \underline{T}_{b,i} \leq T_{b,i} \leq \bar{T}_{b,i} \quad (13)$$

where $\underline{T}_{b,i}$ and $\bar{T}_{b,i}$ represent the lower and the upper limits of equivalent building temperature of subsystem i .

Based on (1) and (2), the maximum flexibility of subsystem i for a period of t_{flexis} can be formulated as

$$\text{Maximize } \int_0^{t_{flexis}} |Q_{flexis,i}(t)| dt \quad (14)$$

subject to

$$(11)-(13)$$

$$\underline{Q}_{h,i} \leq Q_{h,i} \leq \bar{Q}_{h,i} \quad (15)$$

The lower and the upper bounds of output of heat producer i can be expressed as $\underline{Q}_{h,i} = \frac{m_i}{\sum_{i=1}^{N_s} m_i} \underline{Q}_h$, $\bar{Q}_{h,i} = \frac{m_i}{\sum_{i=1}^{N_s} m_i} \bar{Q}_h$.

B. Estimation of Maximum Flexibility Provision

1) Stage I: System Decomposition:

Assume that the DHS includes N_s branch pipelines connected to the same trunk pipeline system. Then the original DHS is divided into N_s subsystems through the following steps:

Step 1.1: Measuring the flow rate m_i at the primary side of the heat substations, where $i=1, 2, \dots, N_s$;

Step 1.2: Decomposing the original DHS into N_s subsystems;

Step 1.3: Calculating the desired output of heat producer i $Q_{d,i}(t)$ and the relevant limits of all subsystems by using (10).

2) Stage II: Subsystem Flexibility Estimation

This stage estimates the maximum available duration of each subsystem at various levels of flexibility provision.

Step 2.1: Estimating the heat demand based on given set-points of building temperature, and calculating $\tau_{d,i}$ by using (9);

Step 2.2: Assuming the supply temperature is operated at T_s^P , then initializing the temperatures of pipelines, heat exchangers and buildings with steady-state estimation values;

Step 2.3: Choosing a suitable time step Δt that is commensurable to $\tau_{d,i}$, and discretizing (11). t_{flexis} is then converted into n_{flexis} steps by $n_{flexis} = t_{flexis}/\Delta t$;

Step 2.4: Dividing $Q_{h,i}$ into n_u intervals and considering $Q_{h,i}$ as a constant during each interval. Set interval $k = 1$;

Step 2.5: Combining the discretized equations with objective (14) and constraints (12), (13), (15) to form a new optimization problem. If the output of the heat producer increases, namely $Q_{h,i}(k) - Q_{d,i}(t_0) > 0$, the objective is expressed as

$$\text{Maximize } \sum_{m=0}^{n_{flexis}} [Q_{h,i}(k) - Q_{d,i}(t_0)] \Delta t \quad (16)$$

If $Q_{h,i}(k) - Q_{d,i}(t_0) < 0$, the objective is expressed as

$$\text{Minimize } \sum_{m=0}^{n_{flexis}} [Q_{h,i}(k) - Q_{d,i}(t_0)] \Delta t \quad (17)$$

The optimization problems for upward and downward regulations of the decomposed subsystems are both linear optimization problems, with $4 \times n_{flex}$ equality constraints and $3 \times n_{flex}$ groups of upper and lower bounds.

Step 2.6: Solving the optimization problem by *fmincon* in MATLAB with the interior-point method to acquire the maximum durations for upward and downward flexibility;

Step 2.7: $k = k+1$, Go to Step 2.5, until $k > n_u$, which indicates the maximum $Q_i(t)$ at all levels of duration F_i are acquired. Then the boundaries of flexibility for subsystem i can be formulated as F_i and Q_i , with a dimension of $1 \times n_u$.

3) Stage III: Flexibility Aggregation

This stage aggregates the maximum duration of subsystems for various levels of flexibility provision.

Since the heat injected into different subsystems are interconnected, the heat producer outputs need to ensure that all subsystems are within limits.

For $Q_{h,i}(k) \geq Q_{d,i}(t_0)$, the upper limit of heat producer i is expressed as

$$Q_{h,i}^{u,lim}(k) = m_i \times \min_{1 \leq i \leq N_s} \left\{ \frac{Q_{h,i}(k)}{m_i} \right\} \quad (18)$$

For $Q_{h,i}(k) < Q_{d,i}(t_0)$, the lower limit of heat producer i is expressed as

$$Q_{h,i}^{l,lim}(k) = m_i \times \max_{1 \leq i \leq N_s} \left\{ \frac{Q_{h,i}(k)}{m_i} \right\} \quad (19)$$

The total flexible output of all subsystems $P_{flexis}(k)$ and the maximum duration $F_{flexis}(k)$ at level k are calculated by

$$F_{flexis}(k) = t_{flexis,k} \quad (20)$$

$$P_{flexis}(k) = \sum_{i=1}^{N_s} [Q_{h,i}^{lim}(k) - Q_{d,i}(k)] / \gamma_{h2p} \quad (21)$$

IV. CASE STUDIES

A radial DHS as shown in Fig. 6 was used to evaluate the performance of the flexibility quantification method. The DHS was coupled to the power grid via a CHP as an example. The rated power of the CHP was 2 MW with a heat to power ratio of 1.333. The minimum power output of the CHP was assumed to be 0 MW. In normal states, the CHP output was controlled to maintain the supply temperature only. The heat produced by the CHP was transported through a trunk pipeline to the joint node and then divided to the two substations. Parameters of pipelines (stainless) in the DHS were listed in Table I.

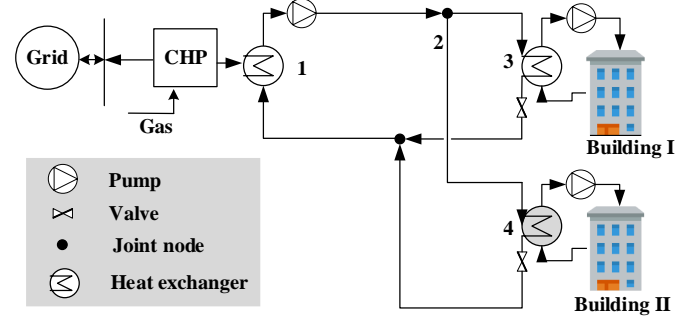


Fig. 6. Schematic of a radial DHS.

TABLE I
PARAMETERS OF THE PIPELINES IN THE DHS

Number	Start	End	Length (m)	Size (mm)
1	1	2	500	DN 200
2	2	3	200	DN 125
3	2	4	500	DN 125

The setpoint of the buildings' temperature was 21°C. The electricity output of CHP in the steady state was 1.305 MW. The supply temperature at the secondary side of the producer heat exchanger is controlled by adjusting the CHP heat output. The supply temperature is limited to be below 99°C. The allowable temperature variation of buildings was between 20°C and 23°C. Heat capacity and heat transfer coefficient of buildings were 225 MJ/°C, 41.2 kW/°C, which were estimated based on the amount of concrete and the level of insulation [37].

A. Model Validation

This case was carried out to show the accuracy of the decomposition method in approximating the behavior of a radial DHS. A commercial simulation software, namely APROS, was used to simulate the behavior of the DHS as a comparison. In the decomposed system, the trunk pipeline was replaced by two pipelines with the same flow rates as the original system. The length of the two pipelines in the subsystems are 0.7 km and 1 km. Two key factors in reflecting the DHS behavior, namely flow rate and temperature, were compared to validate the equivalence of the two models.

To validate that the decomposed system can reflect the dynamic behavior of the original system, the supply temperature was adjusted to different values to observe the response of the whole DHS. The results in Fig. 7 show that the decomposed system approximates the behavior of the original system with a high accuracy.

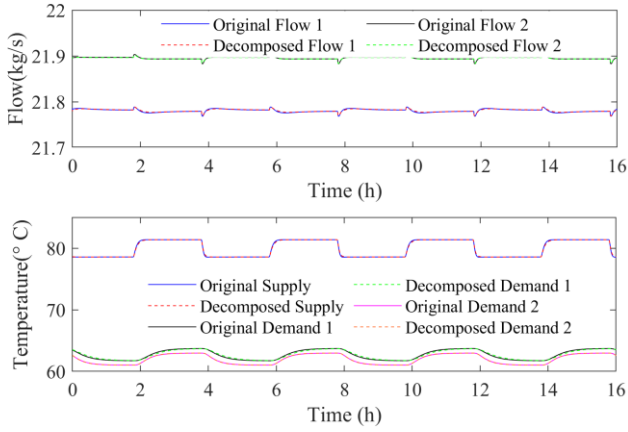


Fig. 7. Simulation results of the decomposed system and the original system.

The upward and the downward flexibility boundaries of the DHS were determined using the proposed method and compared to the flexibility boundaries calculated through simulations of the original DHS. Fig. 8 shows that the decomposed system can approximate the original DHS with respect to flexibility provision. The flexibility boundaries are presented as the maximum change (positive and negative) of CHP electricity output within the allowable duration that ensures all temperatures of the DHS are within limits. The duration refers to the release period of CHP for supporting the power grid. Durations from 30 minutes to 6 hours were considered as an example. The flexibility boundaries were shown as two curves available for upward and downward regulations as shown in Fig. 8. The results also show that the flexibility boundaries shrink as the duration increases. From another perspective, the higher the CHP heat output deviates from the heat demand, the faster the DHS states may go beyond limits.

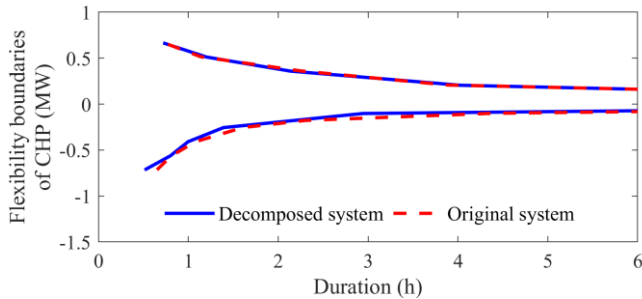


Fig. 8. Flexibility comparison of the decomposed and original systems.

B. Key Factors in Flexibility Quantification

The impacts of system parameters and operating conditions on the upward and the downward flexibility boundaries of the DHS shown in Fig. 6 were discussed in this subsection.

1) Impact of Pipeline Length

To highlight the impact of pipeline length, the flexibility of two simplified DHSs was firstly compared. The lengths of pipelines in the two cases are 1 km and 3 km. Fig. 9 shows the results of this test. Assuming that the demand for flexibility from the power grid emerged at the 5th hour, the CHP electricity output was increased to respond to this demand. As time goes by, the supply temperature in both cases increased. After 1 hour, the demand for flexibility disappeared. The CHP electricity

output was adjusted to restore its heat supply to the DHS. The results show that the supply temperature of the 1 km case increases faster due to a shorter time delay. Meanwhile, a longer period of fluctuation in CHP electricity output and temperature was observed, which may affect the amount of flexibility in DHS for further response.

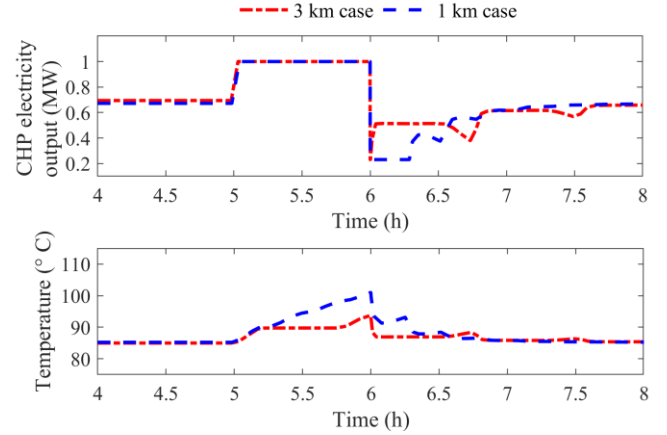


Fig. 9. Variation of electricity output and supply temperature of CHP.

Fig. 10 shows the trajectories of the supply temperature and the building temperature. Although, both systems restored to normal states, the 3 km system was less sensitive to the change of CHP electricity output than the 1 km system. The supply temperature of the 1 km system exceeded its upper bound (99°C) after four cycles, while the temperature of the 3 km system was still within its limits.

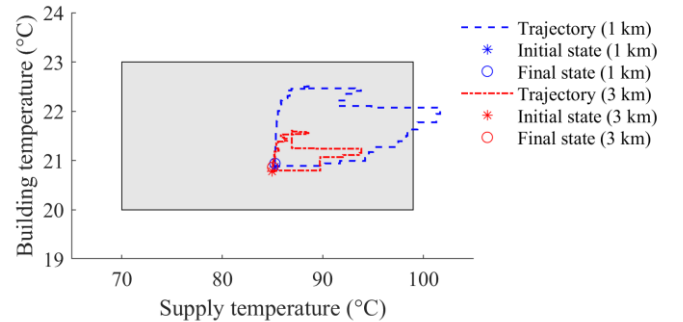


Fig. 10. Variations of supply temperature and building temperature at the DHS.

As shown in Fig. 11, the 3 km system has more flexibility. Both the upward and the downward flexibility boundaries were enlarged at all levels of adjustment in the CHP electricity output. In practice, the DHS may have pipeline networks with tens of kilometers long, which indicates a significant amount of flexibility.

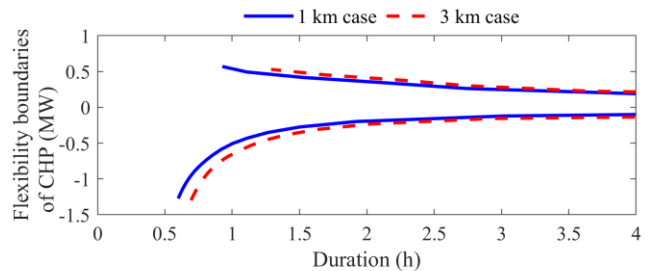


Fig. 11. Impact of pipeline length on the flexibility of the DHS.

2) Impact of Supply Temperature

To investigate the impact of supply temperature on the flexibility provided by the DHS, three studies were performed considering the supply temperatures of 85°C, 90°C and 95°C for the DHS described in Fig. 6 and Table I.

Fig. 12 shows that the available upward flexibility boundary shrinks as the supply temperature goes up. Therefore, the DHS with higher supply temperature reaches its boundary first, which means less upward flexibility can be supplied. This is because higher supply temperature causes the violation of the maximum temperature limits in buildings after a shorter period.

When the supply temperature is within limits, the boundaries of flexibility provision are mainly determined by the building temperature. As a result, the downward flexibility boundaries at different supply temperatures are close to each other.

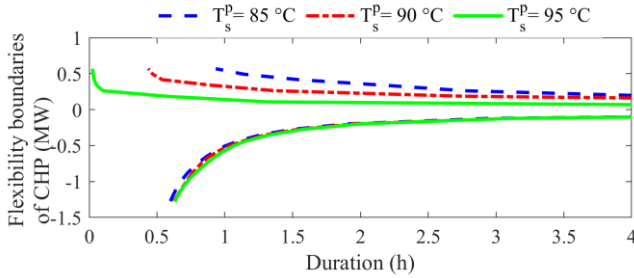


Fig. 12. Flexibility boundaries of the DHS under different supply temperatures.

3) Impact of Thermal Mass and Resistance of Building

In this test, the heat capacity and heat transfer coefficient of buildings were changed to 175 MJ/°C and 31.2 kW/°C separately. The results are shown in Fig. 13. As previously mentioned, the upward flexibility boundary was determined by the supply temperature and the building temperature. The supply temperature is the primary constraint that limits the upward flexibility provision, particularly when the CHP is operated close to its maximum capacity. This is because a high-level heat demand at normal states results in a smaller margin for supply temperature increase. The flexibility of the DHS reached its upper bound before the extra heat caused more impact on the building temperature. As the CHP electricity output decreased, the downward flexibility boundary of the case with 175 MJ/°C heat capacity became smaller than the case with 225 MJ/°C heat capacity.

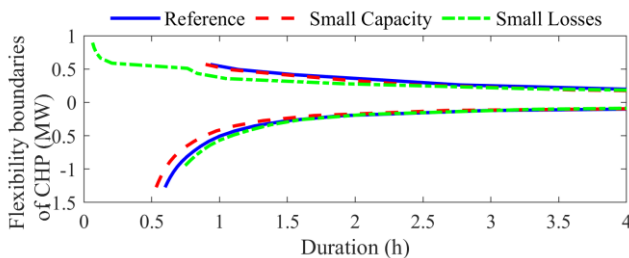


Fig. 13. Flexibility boundaries of the DHS with different building parameters.

For a building with a smaller heat transfer coefficient (well-insulated), the heat demand was lower which indicated that the water flow rate was smaller under the same supply temperature. When the CHP heat output increased, the supply temperature went up faster. As a result, the upward flexibility boundary was smaller than the reference case. Like the previous case with

supply temperature variation, the case with small losses (heat transfer coefficient) has a lower flow rate. The supply temperature affected the downward boundary if the CHP output was below a certain level. Thus, the duration for supporting the demand of flexibility was also shorter than the reference case.

4) Impact of Ambient Temperature

Fig. 14 shows the flexibility boundaries of the DHS with ambient temperatures at -4°C, 0°C and 4°C. In this case, the supply temperature was maintained at 85°C during the normal operation. When the ambient temperature decreased (more heat demand), the flow rate would be at a higher level which indicated that the maximum duration became smaller. This increase led to a decrease of upward flexibility boundary. On the opposite, when the ambient temperature increased, the maximum duration went up. The downward flexibility boundary was thus enlarged. Even though the flow rate was not adjusted during each flexibility calculation process, its value affected the flexibility of the DHS.

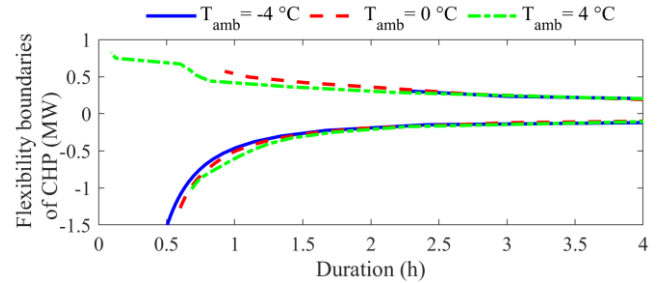


Fig. 14 Flexibility boundaries of the DHS under different ambient temperature.

C. Discussion

The impact of the four key factors on the flexibility of DHSs are summarized in Table II. The results show that the flexibility of DHS is different when system parameters (pipeline length, building insulation, heat capacity) or operating conditions (supply temperature and ambient temperature) are not the same. The findings can support the decision making of DHS owners on flexibility enhancement so that they could make profits from providing flexibility to the power grid.

TABLE II
IMPACT OF DIFFERENT FACTORS ON THE FLEXIBILITY OF DHS

Key factors	Upward flexibility	Downward flexibility
Pipeline length increases	Enlarge	Enlarge
Supply temperature increases	Enlarge	Minor impacts
Building insulation increase	Shrink	Enlarge
Building heat capacity increases	Minor impacts	Enlarge
Ambient temperature increases	Shrink	Enlarge

Note that the implementation of the decomposition method for quantifying the flexibility of the DHS is at the cost of extra steps: 1) Pre-processing: model decomposition and parameter extraction which require prior knowledge on hydraulic and thermal behaviors of the DHS; 2) Post-processing: the aggregation of flexibility of subsystems; 3) Update required for model decomposition when hydraulic conditions change. However, the decomposition method has the following benefits: 1) the computational burden for flexibility quantification of the DHS is reduced; 2) If idle processors exist,

parallel computing can be used to accelerate the problem-solving process, particularly for offline analysis.

By providing flexibility services, the DHS owner can acquire additional profits from the power grid, which vary under different market conditions. Using secondary frequency response in Great Britain as an example, the unit price (per MW) of availability for secondary frequency response is £8.78/h [38]. If 0.5 MW of CHP output is used for secondary frequency response with a tendered duration of 16 h/day, then the CHP owner will receive an estimated payment of £25,637.6/year ($8.78 \times 0.5 \times 16 \times 365$) for being available to provide secondary frequency response.

Note that this paper focuses on the limit of DHS on the CHP, which mainly affects durations that the change of CHP electricity output can sustain. For a given flexibility service requiring fast action, the reserved capacity of CHP is also limited by ramp rates. This limit can be approximated by the minimum response time required by the utility multiplied by the ramp rate of gas-engine used in the CHP. If small gas turbines are used as the engine, the ramp rates typically range between 100 kW/s and 200 kW/s [39]. For a single-shaft gas turbine, this rate could be higher. Using primary frequency response in Great Britain as an example, the CHP needs to reach its full reserved capacity in 10s [29]. Assume that the ramp rate of the gas engine is 100 kW/s, then the maximum reserved capacity that the CHP in this paper can keep for primary frequency response is 1 MW ($100\text{kW/s} \times 10\text{s}$) with respect to ramping limits. As the amplitudes of flexibility boundaries in Fig. 8 are below 1 MW, the ramp rate limit does not change the results of this paper. Besides technical maximum reserve, the reserve capacity is also affected by the forecasting prices of gas and electricity in the energy markets, and the payment from other ancillary services. The CHP owners/operators make decisions about the reserved capacity based on potential benefits over the contract period of ancillary services. A long-term study will be conducted in future to demonstrate the economic benefits providing ancillary services considering the market prices of energy and ancillary services.

V. CONCLUSION

This paper proposed a three-stage methodology to quantify the flexibility of DHSs. The DHSs exchange energy with the power grid through their heat producers' electricity generation/consumption. The behavior of DHSs was approximated by multiple simple DHSs with a single-producer single-consumer structure. The flexibility of the simple DHSs was defined as the maximum duration that the DHS can absorb or release energy within operational limits. An optimal control problem with time delays was formulated to characterize the flexibility boundary of these simple DHSs. A flexibility aggregation method was developed to evaluate the total flexibility of the original DHS. Cumulative flexibility of subsystems enables a simple and portable model to accurately capture the aggregate flexibility of demands, pipelines and the heat producer at a system level.

Case studies showed that the proposed method could represent the flexibility of the original system with high accuracy. The results also showed that the amount of flexibility

of a DHS largely depended on the supply temperature and the building temperature. These states were mainly determined by the supply temperature of the DHS, the heat loss coefficient of buildings, and the ambient temperature.

Some limitations should be noted. Firstly, the decomposition method is not able to analyze a DHS with a ring-shaped pipeline network or multiple heat producers directly. Secondly, the proposed method is not suitable for a DHS using variable flow control to maintain the heat supply. Thirdly, details of secondary pipeline networks are not considered in this paper. The proposed approach is only validated by a small-scale radial DHS. But it can be extended to large-scale systems from two aspects: 1) For a radial DHS with a large number of pipelines and customers, a simplified structure can be extracted by aggregating of pipelines and demands of DHSs; 2) For a ring-shaped DHS with multiple heat producers, the DHS can be divided into multiple radial networks at hydraulic intersection users or common pipe branches. Then the proposed approach can be applied to each divided system's flexibility analysis.

APPENDIX

A. Model of the DHS

1) *Pipeline Model*: When the DHS is used for flexibility services, the fast electricity fluctuation is transferred to the DHS. To avoid evident pressure changes, the flow rate is not adjusted during the flexibility provision process. As hydraulic dynamics are much faster than thermal dynamics, a quasi-dynamic pipeline model was used to describe the transport delay effect [40]

$$\begin{aligned} T_{out}(t) &= f_p(T_{in}(t - \tau_d)) \\ &= T_{in}(t - \tau_d) \times e^{-\frac{\lambda L}{c_w \dot{m}}} + T_{env} \times \left(1 - e^{-\frac{\lambda L}{c_w \dot{m}}}\right) \end{aligned} \quad (22)$$

where $T_{in}(t)$ and $T_{out}(t)$ are inlet and output temperatures of the pipeline. f_p is the thermal model of the pipeline. λ and L are overall heat transfer coefficient and length of the pipeline. \dot{m} is the flow rate of the pipeline. c_w is the specific heat of water.

2) *Heat exchanger*: In the flexibility analysis, the energy transfer function of the heat exchanger is concerned. So, a simplified model is used to describe the thermal dynamics of the heat producer side system [41]

$$c_w m_2^p \frac{dT_s^p}{dt} = Q_h - c_w \dot{m}_p (T_s^p - T_r^p) \quad (23)$$

where T_r^p and \dot{m}_p are return temperature and flow rate at the secondary side of the heat exchanger. m_2^p is the mass of water inside the heat exchanger.

At the building side, the heat is absorbed from the primary network through a heat exchanger, which is modeled by

$$\begin{cases} c_w m_1^b \frac{dT_{1,o}^b}{dt} = c_w \dot{m}_p (T_{1,i}^b - T_{1,o}^b) - H^b (T_{1,o}^b - T_{2,o}^b) \\ c_w m_2^b \frac{dT_{2,o}^b}{dt} = H^b (T_{1,o}^b - T_{2,o}^b) - c_w \dot{m}_b (T_{2,o}^b - T_b) \end{cases} \quad (24)$$

where $T_{1,i}^b$ and $T_{1,o}^b$ are inlet and output temperatures at the primary side of the heat exchanger. $T_{2,i}^b$ and $T_{2,o}^b$ are inlet and output temperatures at the secondary side of the heat exchanger. m_1^b and m_2^b are the mass flow inside primary and secondary circuits of the heat exchanger. H^b is the heat loss coefficient of

the heat exchanger.

3) *Building*: A simple lumped parameter model was used to describe a building's energy behavior [37]. Assume that no other heat sources are used, then the building is modeled as

$$C_b \frac{dT_b}{dt} = c_w \dot{m}_b (T_{2,o}^b - T_b) - k_l (T_b - T_{amb}) \quad (25)$$

where C_b is the heat capacity of the building. \dot{m}_b is the flow rate of the secondary side of the building heat exchanger. k_l is the overall heat loss coefficient. C_b and k_l are empirical values, which can be estimated by identifying building behaviors [37].

B. Thermal Inertia of Water in Pipeline and Building

Referring to (23), the desired heat output of CHP at t_0 can be expressed as $Q_d = c_w \dot{m}_p (T_s^p(t_0) - T_r^p)$ when the DHS is operated at the steady state. When supporting the power grid by changing the electricity output, the heat output of CHP is changed to $Q_h = Q_d + \gamma_{h2p} P_{flexis}$. The general solution of the heat supply system at the producer side (23) is expressed as

$$T_s^p(t) = \frac{Q_h + c_w \dot{m}_p T_r^p}{c_w \dot{m}_p} - \frac{Q_h - Q_d}{c_w \dot{m}_p} e^{-\frac{\dot{m}_p}{m_2^p}(t-t_0)} \quad (26)$$

Heat supply to the buildings is not affected by the changes in the heat output until water flows from the producer side to the demand side with a transport delay τ_d .

For upward regulation (increasing CHP output), the flexibility requested by the power grid is below the upward boundary, namely $0 \leq P_{flexis} \leq \bar{P}_{flexis}$. Then $\forall t \in (t_0, t_0 + \tau_d]$,

$$T_s^p(t) \leq \frac{Q_h + c_w \dot{m}_p T_r^p}{c_w \dot{m}_p} = \frac{Q_d + \gamma_{h2p} \bar{P}_{flexis} + c_w \dot{m}_p T_r^p}{c_w \dot{m}_p} \leq \frac{Q_d + \gamma_{h2p} \bar{P}_{flexis} + c_w \dot{m}_p T_r^p}{c_w \dot{m}_p} \quad (27)$$

To ensure the security of the DHS, the supply temperature is limited below \bar{T}_s^p . If \bar{P}_{flexis} satisfies $\frac{Q_d + \gamma_{h2p} \bar{P}_{flexis} + c_w \dot{m}_p T_r^p}{c_w \dot{m}_p} \leq \bar{T}_s^p$, the DHS can accommodate an increase in the CHP electricity output \bar{P}_{flexis} for at least a period of τ_d before the higher temperature water reaches the building side.

For downward regulation (decreasing CHP output), a drop of supply temperature will be observed due to less heat supply. But the water in the supply pipeline will keep heating the building for another period τ_d . Even if the heat supply at the producer side is reduced to zero, the building temperature can sustain for at least τ_d due to the thermal inertia of the building. Besides, the building can maintain its temperature at a level above the minimum temperature \underline{T}_b for another period t_b due to the thermal inertia of the building. Without heat input, the general solution of the building side system (25) is expressed as

$$T_b(t) = T_{amb} - (T_{amb} - T_b(t_0)) e^{-\frac{k_l}{C_b}(t-t_0)} \quad (28)$$

It can be obtained that $t_b = \frac{C_b}{k_l} \ln \left(\frac{T_b(t_0) - T_{amb}}{\underline{T}_b - T_{amb}} \right) + t_0$. Therefore, the DHS can accommodate a decrease in the electricity output for at least a period of $\tau_d + t_b$.

C. Computational Complexity Analysis

In this paper, the interior-point method was used for solving both the original problem and the equivalent problem. Regarding computational complexity, the key difference of the two models lies in the dimension of dynamic constraints after differencing. To show the benefits, the original model and the equivalent model are compared as follows.

For simplicity, the Euler method was used to discretize the models. The discretized equation of the original system (3) can be expressed as

$$\frac{\mathbf{T}(t + \Delta t) - \mathbf{T}(t)}{\Delta t} = f(t, \mathbf{T}(t), \mathbf{T}(t - n_{p,1}\Delta t), \mathbf{T}(t - n_{p,2}\Delta t), \dots, \mathbf{T}(t - n_{p,N_p}\Delta t), Q_h, \mathbf{T}_w) \quad (29)$$

where $n_{p,1} = \frac{\tau_1}{\Delta t}$, $n_{p,2} = \frac{\tau_2}{\Delta t}$, ..., $n_{p,N_p} = \frac{\tau_{N_p}}{\Delta t}$. Δt is the step size, which satisfies that $n_{p,1}, n_{p,2}, \dots, n_{p,N_p}$ are integers within the allowable tolerance range.

Combined with (6), the above model can be reformulated as the standard form of linear programming. Considering delayed variables, the dimension of variables in the standard-form can be $n_{ori} = (N_p + 1) \times N_T$ in the worst case. The computational complexity of the original system is thus no more than $O(n_{ori}^3 L)$ where L is integer data of bit size [42].

Assume that Δt is also used for the equivalent model, the discretized equation of subsystem (11) can be expressed as

$$\frac{\mathbf{T}_i(t + \Delta t) - \mathbf{T}_i(t)}{\Delta t} = \mathbf{A}_0 \mathbf{T}_i(t) + \mathbf{A}_1 \mathbf{T}_i(t - n_{d,i}\Delta t) + \mathbf{B} Q_{h,i}(t) + \mathbf{E} \mathbf{T}_w \quad (30)$$

Considering delayed variables, the dimension of variables in the standard form can be $n_{eq,i} = 2 \times 4$ in the worst case. The computational complexity of the original system is thus no more than $O(n_{eq,i}^3 L)$.

For a real DHS, N_T is the temperature variables of the whole system, which satisfies $N_T > 4$. The number of pipelines satisfies $N_p > 2$. Therefore, it can be concluded that $O(n_{ori}^3 L) \gg O(n_{eq,i}^3 L)$.

The flexibility analysis of the subsystems in the equivalent model needs to be conducted for N_s (the number of subsystems) times. As N_s is smaller than N_p , the complexity of the proposed approach based on the equivalent model is still much lower than the complexity of the original model.

Note that if other difference methods, such as 4th order Runge-Kutta method, are used, the complexity could be 4 times higher, which indicates the complexity difference between the original model and the equivalent model could be even higher.

D. Parameter Extraction of the Decomposed Subsystem

The decomposition process includes two aspects: 1) Hydraulic decomposition based on graph theory and Kirchhoff's Law, which ensures that the pressure drop along the decomposed pipelines is equivalent to the pressure drop of the original pipeline; 2) Thermal decomposition, which ensures the temperature drop of the decomposed pipelines and the original pipeline are the same. The equivalent of the heat transfer coefficient of the decomposed pipeline is analogous to the equation used for calculating the friction factors of the

decomposed pipelines.

1) Equivalent Friction Factor for Hydraulic Decomposition

The equivalent friction factor of the decomposed pipeline is extracted from the friction factor of the original pipeline by

$$f_{i,j} = f_i \frac{D_{i,j}}{D_i} \quad (31)$$

where $f_{i,j}$ is the friction factor of the j^{th} decomposed pipeline of the original pipeline i . f_i is the friction factor of the original pipeline i . $D_{i,j}$ is the diameter of the j^{th} decomposed pipeline of pipeline i . D_i is the diameter of pipeline i .

Describe the pressure drop of the j^{th} decomposed pipeline as

$$\Delta H_{i,j} = f_{i,j} \frac{L_i}{D_{i,j}} \rho \frac{v_i^2}{2} \quad (32)$$

Then the pressure drops of the decomposed pipelines and the original pipeline satisfy

$$\Delta H_i = \Delta H_{i,1} = \Delta H_{i,2} = \dots = \Delta H_{i,n_i} \quad (33)$$

2) Heat Loss Factor for Thermal Decomposition

The equivalent of the heat transfer coefficient of the decomposed pipeline is extracted from the heat transfer coefficient of the original pipeline by

$$\lambda_{i,j} = \lambda_i \frac{D_{i,j}^2}{D_i^2} \quad (34)$$

where λ_i is the heat transfer coefficient of pipeline i . $\lambda_{i,j}$ is the heat transfer coefficient of the j^{th} decomposed pipeline of pipeline i .

Describe the temperature drop of the pipelines by using (22), then heat losses of the decomposed pipelines and the original pipeline satisfy

$$T_{out,i} = T_{out,i,1} = T_{out,i,2} = \dots = T_{out,i,n_i} \quad (35)$$

E. Parameters of the DHS Model

$$\mathbf{A}_0 = \begin{bmatrix} -\frac{\dot{m}_p}{m_2^p} & 0 & 0 & 0 \\ 0 & -\frac{\dot{m}_p}{m_1^b} - \frac{H^b}{c_w m_1^b} & \frac{H^b}{c_w m_1^b} & 0 \\ 0 & \frac{H^b}{c_w m_2^b} & -\frac{H^b}{c_w m_2^b} - \frac{\dot{m}_b}{m_2^b} & \frac{\dot{m}_b}{m_2^b} \\ 0 & 0 & \frac{c_w \dot{m}_b}{c_b} & -\frac{c_w \dot{m}_b}{c_b} - \frac{k_l}{c_b} \end{bmatrix}$$

$$\mathbf{A}_1 = \begin{bmatrix} 0 & \frac{\dot{m}_p}{m_2^p} e^{-\frac{\lambda L}{c_p \dot{m}_p}} & 0 & 0 \\ \frac{\dot{m}_p}{m_1^b} e^{-\frac{\lambda L}{c_p \dot{m}_p}} & 0 & 0 & 0 \\ 0 & 0 & 0 & 0 \\ 0 & 0 & 0 & 0 \end{bmatrix}$$

$$\mathbf{B} = \begin{bmatrix} \frac{1}{c_w m_2^p} \\ 0 \\ 0 \\ 0 \end{bmatrix}, \mathbf{E} = \begin{bmatrix} \frac{\dot{m}_p}{m_2^p} \left(1 - e^{-\frac{\lambda L}{c_p \dot{m}_p}}\right) & 0 \\ \frac{\dot{m}_p}{m_1^b} \left(1 - e^{-\frac{\lambda L}{c_p \dot{m}_p}}\right) & 0 \\ 0 & 0 \\ 0 & \frac{k_l}{c_b} \end{bmatrix}$$

REFERENCES

- [1] "System price peak highlights UK power generation market complexity." [Online]. Available: <http://www.powerengineeringint.com/articles/2017/06/system-price-peak-highlights-uk-power-generation-market-complexity.html>. Access on: Dec. 21, 2018.

- [2] E. Dall'Anese, P. Mancarella, and A. Monti, "Unlocking flexibility: integrated optimization and control of multi-energy systems," *IEEE Power Energy M.*, vol. 15, pp. 43-52, Jan. 2017.
- [3] H. Sun, Q. Guo, B. Zhang, W. Wu, B. Wang, X. Shen, and J. Wang, "Integrated energy management system: concept, design, and demonstration in China," *IEEE Electrification Mag.*, vol. 6, no. 2, pp. 42-50, May 2018.
- [4] P. Mandatova, and O. Mikhailova, Flexibility and aggregation: requirements for their interaction in the market. Eurelectric: Brussels, Belgium. 2014. [Online]. Available: <https://www.usef.energy/app/uploads/2016/12/EUR-ELECTRIC-Flexibility-and-Aggregation-jan-2014.pdf>. Access on: Dec. 21, 2018.
- [5] W. Gu, J. Wang, S. Lu, Z. Lu, and C. Wu, "Optimal operation for integrated energy system considering thermal inertia of district heating network and buildings," *Appl. Energy*, vol. 199, pp. 234-246, Aug. 2017.
- [6] A. Vandermeulen, B. Heijde, and L. Helsen, "Controlling district heating and cooling networks to unlock flexibility: A review," *Energy*, vol. 151, pp. 103-115, May 2018.
- [7] D. M. Sneum, E. Sandberg, E. R. Soysal, K. Skytte, and O. J. Olesen, "Framework conditions for flexibility in the district heating-electricity interface," Flex4Res Proj, 2016. <http://www.nordicenergy.org/wp-content/uploads/2016/10/Flex4-RES-WP2-DH-report.pdf>. Access on: Dec. 21, 2018.
- [8] N. G. Paterakis, O. Erdin, and J. P. Catalão, "An overview of demand response: key-elements and international experience," *Renew. Sustain. Energy & Reviews*, vol. 69, pp. 871-91, Mar. 2017.
- [9] B. J. Claessens, D. Vanhoudt, J. Desmedt, and F. Ruelens, "Model-free control of thermostatically controlled loads connected to a district heating network," *Energy & Buildings*, vol. 159, pp.1-10, Jan. 2018.
- [10] J. G. Kirkerud, T. F. Bolkesjø, and E. Trømborg, "Power-to-heat as a flexibility measure for integration of renewable energy," *Energy*, vol. 128, pp.776-784, Jun. 2017.
- [11] Y. Dai, L. Chen, Y. Min, Q. Chen, K. Hu, J. Hao, Y. Zhang, and F. Xu, "Dispatch model of combined heat and power plant considering heat transfer process," *IEEE Trans. Sustain. Energy*, vol. 8, no. 3, pp:1225-36, Jul 2017.
- [12] Z. Li, W. Wu, M. Shahidehpour, J. Wang, and B. Zhang, "Combined heat and power dispatch considering pipeline energy storage of district heating network," *IEEE Trans. Sustain. Energy*, vol. 7, no. 1, pp. 12-22, Jan. 2016.
- [13] F. Verrilli, S. Srinivasan, G. Gambino, M. Canelli, M. Himanka, C. Del Vecchio, M. Sasso, and L. Glielmo, "Model predictive control-based optimal operations of district heating system with thermal energy storage and flexible loads," *IEEE Trans. Autom. Sci. Eng.*, vol. 14, no. 2, pp. 547-557, April 2017.
- [14] "Reciprocating engines: Giving wind farm reliability a lift," Power Engineering International, 2007. [Online]. Available: <https://www.powerengineeringint.com/articles/print/volume-15/issue-7/features/reciprocating-engines-giving-wind-farm-reliability-a-lift.html>. Access on: Dec. 01, 2019.
- [15] D. Jones, M. Kelly, "Supporting Grid Modernization with Flexible CHP Systems," ICF [Online], Nov 2017. Available: <https://www.icf.com/resources/white-papers/2017/supporting-grid-modernization-with-flexible-chp-systems>. Access on: Nov. 10, 2019.
- [16] T. Korpela, J. Kaivosoja, Y. Majanne, L. Laakkonen, M. Nurmoranta, and M. Vilkkö, "Utilization of district heating networks to provide flexibility in CHP production," *Energy Procedia*, vol. 116, pp. 310-319, Jun 2017.
- [17] J. Riveros, R. Donceel, J. Van Engeland, and W. D'haeseleer, "A new approach for near real-time micro-CHP management in the context of power system imbalances—A case study," *Energ. Conv. & Mana.* vol. 89, pp. 270-80, Jan. 2015.
- [18] J. G. Kirkerud, T. F. Bolkesjø, and E. Trømborg, "Power-to-heat as a flexibility measure for integration of renewable energy," *Energy*. vol. 128, pp. 776-784, Jun. 2017.
- [19] Z. Li, W. Wu, J. Wang, B. Zhang, and T. Zheng, "Transmission-constrained unit commitment considering combined electricity and district heating networks," *IEEE Trans. Sustain. Energy*, vol. 7, no. 2, pp. 480-492, Apr. 2016.

- [20] H. Madsen, K. Sejling, H. T. Sogaard, and O. P. Palsson, "On flow and supply temperature control in district heating systems," *Heat. Recovery Syst. & CHP*, vol. 14, no. 6, pp. 613-620, Nov. 1994.
- [21] M. Chertkov, and N. N. Novitsky, "Thermal transients in district heating systems," *Energy*, in-press. <https://doi.org/10.1016/j.energy.2018.01.049>
- [22] Z. Pan, Q. Guo, and H. Sun, "Feasible region method based integrated heat and electricity dispatch considering building thermal inertia," *Appl. Energy*, vol. 192, pp. 395-407, Apr. 2017.
- [23] M. J. Sanjari, H. Karami, and H. B. Gooi, "Analytical rule-based approach to online optimal control of smart residential energy system," *IEEE Trans. Ind. Inform.*, vol. 13, no. 4, pp. 1586-1597, Aug 2017.
- [24] S. Grosswindhager, A. Voigt, and M. Kozek, "Efficient physical modeling of district heating networks," in *Proc. Modeling and Simulation*, Calgary, AB, Canada, 2011.
- [25] C. Wu, W. Gu, P. Jiang, Z. Li, H. Cai, and B. Li, "Combined economic dispatch considering the time-delay of a district heating network and multi-regional indoor temperature control," *IEEE Trans. Sustain. Energy*, vol. 9, pp.118-127, Jan 2018.
- [26] Y. Dai, L. Chen, Y. Min, Q. Chen, J. Hao, K. Hu, and F. Xu, "Dispatch model for CHP with pipeline and building thermal energy storage considering heat transfer process," *IEEE Trans. Sustain Energy*, vol. 10, no. 1, pp. 1361-72, Jan 2019.
- [27] L. Zhao, W. Zhang, H. Hao and K. Kalsi, "A geometric approach to aggregate flexibility modeling of thermostatically controlled loads," *IEEE Trans. Power Systems*, vol. 32, no. 6, pp. 4721-4731, Nov. 2017.
- [28] S. Kundu, K. Kalsi and S. Backhaus, "Approximating flexibility in distributed energy resources: a geometric approach," *2018 Power Systems Computation Conference (PSCC)*, Dublin, 2018, pp. 1-7.
- [29] National Grid. Firm Frequency Response (FFR) Interactive Guidance. 2017. [Online]. Available: <https://www.nationalgrideso.com/balancing-services/frequency-response-services/firm-frequency-response-ffr>. Access on: Oct 27, 2019.
- [30] National Grid. Short Term Operating Reserve (STOR) Interactive Guidance. 2018. [Online]. Available: <https://www.nationalgrideso.com/balancing-services/reserve-services/short-term-operating-reserve-stor?technical-requirements..> Access on: Dec. 21, 2018.
- [31] S. Frederiksen, and S. Werner. District heating and cooling. Studentlitteratur; 2013.
- [32] S. C. Bhatia, Advanced renewable energy systems, WPI Publishing, 2014.
- [33] R. B. Vinter, "State constrained optimal control problems with time delays," *Journal of Mathematical Analysis and Applications*, vol. 457, no. 2, pp. 1696-712, Jan. 2018.
- [34] X. Liu, J. Wu, N. Jenkins, and A. Bagdanavicius, "Combined analysis of electricity and heat networks," *Appl. Energ.*, vol. 162, pp. 1238-1250, Jan. 2016.
- [35] Siemens. PSS sincal 7.0 heating manual; 2010.
- [36] P. Urone, and R. Hinrichs, College physics. OpenStax. 2012. [Online]. Available: <https://openstax.org/details/books/college-physics>. Access on: Aug. 22, 2019.
- [37] J. Hedbrant, "On the thermal inertia and time constant of single-family houses," Dept. Mecha. Eng., Ph.D. dissertation, Linköpings University, Linköping, Sweden. 2001.
- [38] M. Cheng, S. Sami, and J. Wu, "Benefits of using virtual energy storage system for power system frequency response," *Applied Energy*, vol. 194, pp. 376-385, May 2017.
- [39] M. Welch, and A. Pym, "Improving the Flexibility and Efficiency of Gas Turbine-Based Distributed Power Plants", *Power Engineering*, vol. 119, no. 9, Sep. 2015. Available: <https://www.power-eng.com/2015/09/14/improving-the-flexibility-and-efficiency-of-gas-turbine-based-distributed-power-plants/#gref>. Access on: Dec. 01, 2018.
- [40] sisHYD V8i, Bentley Systems, Incorporated. Exton, PA USA, 2012.
- [41] N. M. Abbasov, R. I. Zeinalov, O. M. Azizova, and S. N. Imranova, "Dynamic models of heat exchangers," *Chem. Technol. Fuels Oils*, vol. 42, no. 1, pp. 25-29, Jan. 2006.
- [42] K. Anstreicher, J. Ji, F. Potra, and Y. Ye, "Probabilistic analysis of an infeasible-interior-point algorithm for linear programming," *Mathematics of Operations Research*, vol. 24, no. 1, pp. 176-192, Feb. 1999.



Xiandong Xu (M'15) received the B.Sc. and Ph.D. degrees in electrical engineering from Tianjin University, China, in 2009 and 2015, respectively.

He is currently a Research Associate at Cardiff University, UK. His research focuses on modelling and flexibility analysis of integrated energy systems, and decarbonization of heat through a whole energy systems approach.



Quan Lyu (M'15) received the B.Sc. and Ph.D. degrees in electrical engineering from Dalian University of Technology, China, in 2002 and 2008, respectively.

Currently, he is an Associate Professor at Dalian Institute of Technology. His research focus on planning and market-oriented operation of integrated energy systems with high-penetration renewable energy.



Meysam Qadrdan (M'13) received the B.Sc. degree in Physics from Ferdowsi University of Mashhad, Iran, the M.Sc. degree in Energy Systems Engineering from Sharif University of Technology, Iran, and the Ph.D. degree in Electrical Engineering from Cardiff University, U.K., in 2005, 2008, and 2012, respectively.

Currently, he is a Reader at Cardiff University. His research looks at modelling and optimization of integrated energy systems including electricity, gas and heat.



Jianzhong Wu (M'04) received his B.S., M.S. and Ph.D. degrees in electrical engineering from Tianjin University, China, in 1999, 2002 and 2004, respectively.

He is currently a Professor of Multi-Vector Energy Systems and Head of Department of Electrical and Electronic Engineering at Cardiff University, UK. His research interests include energy infrastructure and smart grid.

Prof. Wu is a Subject Editor of Applied Energy. He is the Director of Applied Energy UNILAB on Synergies between Energy Networks. He is a co-Director of UK Energy Research Centre and EPSRC Supergen Hub on Energy Networks.